2014 IEEE/ASME International Conference on
Advanced Intelligent Mechatronics (AIM)
Besançon, France, July 8-11, 2014

Introduction of a LIDAR-Based Obstacle Detection System on the LineScout Power Line Robot

Pierre-Luc Richard, *Member IEEE,* Nicolas Pouliot and Serge Montambault, *Member IEEE*

***Abstract* – This paper is a sequel of an earlier paper that featured a thorough characterization of the Hokuyo UTM-30LX laser range finder, which showed promise for a specific application: allowing a power line robot to detect obstacles in its path. After a quick summary of the earlier conclusions, this paper pushes the validation farther by assessing for the first time this popular LIDAR's performance when subjected to the particularly challenging, outdoor, power line environmental conditions: large temperature range, changes in lighting, strong magnetic fields, and oscillating or vibrating targets. Use of return signal intensity, predictably affected by the angle of incidence on the target and by target surface finish, is also investigated as a means to detect variations due to an obstacle. Scanning results with LineScout traveling at maximum speed on a full-scale power line span are then analyzed to validate the proposed detection thresholds.**

Keywords – Field robotics; telerobotics; power line inspection robot; LIDAR

I. Introduction

Laser range finders (LIDARs) are widely used in mobile robotic systems for obstacle detection and environment mapping. Though initially such systems were bulky and mostly used for indoor applications, today's miniature LIDAR systems like the Hokuyo UTM-30LX are compact, light, less expensive and robust enough in some cases to work in sunlight, dust, rain and other outdoor conditions [1].

Today, such small, powerful units equip a plethora of outdoor mobile robots and have proven their performance in various environments and for various types of obstacles: on paved roads [2], on rural roads [3], in dense forest [4], through crowds of pedestrians [5], for detecting river banks [6], for avoiding crops in fields [7] and for scanning simulated extraterrestrial terrain [8].

Meanwhile, power line robots (PLRs) for inspection or maintenance tasks are being developed throughout the world [9]. None of this emerging type of outdoor mobile robot is known to be using LIDAR to detect obstacles. So far, the documented means that PLRs use to scan their specific environment are arrays of ultrasonic proximity sensors [10],[11], combined with IR imaging [12], image processing using 2D feature recognition [13],[14],[15] and magnetic field sensors that map the density around energized line components [16].

LineScout Technology, shown in Figure 1, was introduced as a teleoperated PLR in 2006 [17]. It relies on visual feedback transmitted to the operator to detect obstacles. The control strategy then requires that the operator input commands to LineScout so that it can clear the obstacles using its five degrees of freedom [18]. This strategy was instrumental in minimizing development time, easing the introduction of LineScout within the power utility community, and allowing the collection of valuable field results on dozens of major spans [19].

Figure 1. LineScout power line robot on a full-scale power line mockup.

The LineScout project has now entered a new phase of development. Autonomous navigation systems are gradually introduced as additional sensors and feedback devices are implemented onto the moving platform, enabling it to perform autonomous actions, therefore relieving the operator of navigation and obstacle-crossing chores. Towards that goal, this paper builds on previously presented work [20], which defines the objectives and explains why the Hokuyo UTM-30LX was selected as the main detection sensor.

The earlier paper presented a thorough characterization of the sensor in the specific context of scanning cylindrical objects at close range (500 to 1,500 mm). The sensor's potential was confirmed since distance measurement precision and standard deviation under laboratory conditions were found to be satisfactory. Furthermore, continuously evaluating the scanned diameter appeared to be effective in detecting any relevant *change* of diameter of the conductor (typically 30 mm), possibly due to the presence on the line of vibration dampers, suspension clamps or even cable splices, which increase the diameter by only 10 mm (see Figure 2).

Pierre-Luc Richard is with Hydro-Québec's Research Institute (IREQ), Varennes, Québec, Canada, J3X 1S1 (e-mail: richard.pierre-luc@ireq.ca)
Nicolas Pouliot is with Hydro-Québec's Research Institute (IREQ), Varennes, Québec, Canada, J3X 1S1 (e-mail: pouliot.nicolas@ireq.ca).
Serge Montambault is with Hydro-Québec's Research Institute (IREQ), Varennes, Québec, Canada, J3X 1S1 (e-mail: montambault.serge@ireq.ca)

Authorized licensed use limited to: Universidade Tecnologica Federal do Parana. Downloaded on January 22,2025 at 11:01:11 UTC from IEEE Xplore. Restrictions apply.

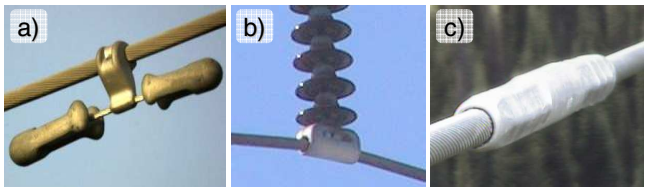

Figure 2. Power line components: a) vibration damper, b) suspension clamp, c) cable splice.

In this paper's Section II, the LIDAR's performance is further assessed when subjecting it to challenging conditions in a typical power line environment: large temperature range, changes in lighting and strong magnetic fields. The use of return signal intensity, predictably affected by the angle of incidence on the target and target surface finish, is also investigated as a source of information since a sudden variation in intensity could indicate an obstacle. Section III discusses thresholds for determining obstacles, with an emphasis on the effect of scanning an oscillating or vibrating target while evaluating its perceived diameter. It then presents the very first series of outdoor LIDAR experiments run with a simple PLR (LineROVer) on a cable. Section IV describes tests with LineScout traveling at maximum speed on a full-scale power line mockup in order to validate the detection thresholds proposed for three different variables. The successful results obtained through this comprehensive and unique set of realistic conditions tests allowed to consider the project's next phases, that are outlined in Section V as a conclusion.

I. Characterization of the Environment

This section presents the effect of three environmental parameters on distance and diameter measurements. A representative specimen of clean cable is placed perpendicular to the LIDAR at a reference distance of L = 1,000 mm. This target is then scanned 2,000 times and the cable's edges are determined using maximum and minimum slopes (distance vs. angle) for each scan. The target's center is then found and the corresponding data point is set as the perceived distance from LIDAR, L_m. Also, the number of laser points n that hit the target is used to determine the perceived diameter D_0 by multiplying it by $L_m \cdot r$, where r is the LIDAR's linear resolution at distance L_m. As an example, given an angular resolution of 0.25 degrees, r equals 4.4 mm when L_m = 1,000 mm. This is similar to the method used in [21] for the specific case where $L_m >> D_0$ (1 m >> 0.03 m). This is satisfactory since the diameter variation is more important than the real value of the diameter.

A. Temperature

As LineScout is used both in winter and summer, it is subjected to a large range of temperatures. Temperature-controlled rooms were thus used to test the LIDAR at -10ºC, 0ºC, 22ºC and 40ºC. All temperatures were maintained within ±1ºC. To avoid any heat loss due to forced convective effect generated by fans inside the rooms, the LIDAR and targets were enclosed during the tests, which were run in the dark so that lighting could not affect measurements. Overall, 2,000 measurements were made after having left the test setup inside each room for a few hours so that the temperature could stabilize [20]. Results are presented as histograms, like those in Figure 3.

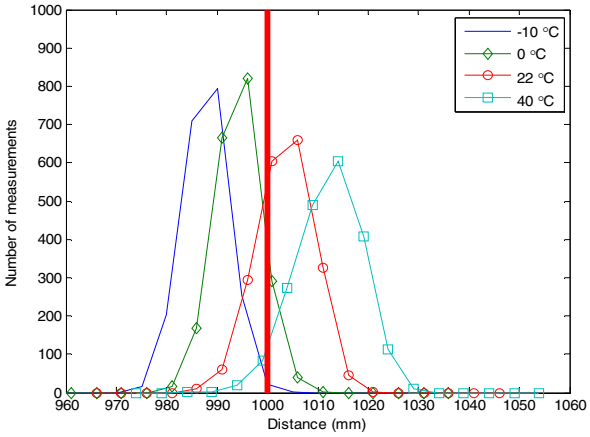

Figure 3. Effect of temperature on the distance measurement.

The selected temperature range is aligned with LineScout typical operating range and it appears to be enough to conclude that temperature significantly affects distance measurements, mean distance values for the clean cable as the temperature increases being 989.9, 996.3, 1005.5 and 1014.3 mm. Such behavior is nearly linear within the range tested. The relative error ε, given by Eq. (1), varies between 0.4% and 1.4%, which is significant compared to all room temperature tests made in [20].

$$|\varepsilon| = \left|\frac{\mu - L}{L}\right| \times 100 \,. \tag{1}$$

In Eq. (1) μ is the mean value and L is the reference distance (1,000 mm).

Although standard deviation σ remains low, it does increase slightly with temperature, from 4.2 to 6.3 mm. Such values remain within manufacturer performance specifications (σ< 10 mm under 3,000 lx and 10 m for a white Kent sheet) but working in extreme temperatures may lead to greater error values. For temperatures below 22ºC, perceived diameter D_0 remains fairly constant: 30.2 and 30.7 mm with a standard deviation of 0.7 mm. However, tests at 40ºC result in a perceived diameter of 39.3 mm. This difference is caused by two more points actually hitting the cable, with a linear resolution of 4.4 mm, suggesting that high temperatures may increase LIDAR beam dispersion. To learn more about this behavior, measurements were made in a room at 22ºC with a close background after heating only the target to over 50ºC, a temperature that an energized high-power transmission cable may typically reach. In this case, no effect on the diameter measurement was noted, meaning that it is probably warming of the LIDAR and not the target that increases sensitivity.

B. Effect of Lighting

In addition to extreme temperatures, outdoor work with LineScout implies various lighting conditions, often quite unlike indoor test conditions. Direct sunlight can affect distance measurements, even manufacturers of UTM-30LX

Authorized licensed use limited to: Universidade Tecnologica Federal do Parana. Downloaded on January 22,2025 at 11:01:11 UTC from IEEE Xplore. Restrictions apply.

do not guarantee performance up to specifications under such conditions. The LIDAR was therefore tested both in direct sunlight and shaded from the sun. For comparison, tests were also run in a lighted room (< 3,000 lx) and a darkened room. Figure 4 presents the results for all tests, which were conducted at 23ºC.

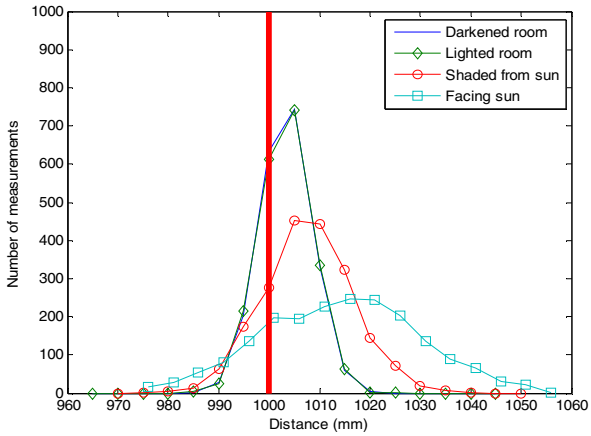

Figure 4. Effect of lighting on the distance measurement.

Results reveal that lighting conditions greatly affect the distance measurement. For a cable, the systematic error ε increases from 0.6% to 1.7% as light increases (curves peak farther to the right). The standard deviation also increases significantly, from 4.9 to 16.1 mm (wider bell curves).

An interesting fact concerns the perceived diameter, which remains fairly constant (39.3 and 39.9 mm) regardless of lighting conditions, although the standard deviation does increases somewhat (from 0.2 to 0.6 mm) due to the distance measurement error. Overall, diameters are greater than for tests in the previous section. This is explained by the effect of a close-range background on laser beam edge detection, called the "mixed pixel effect" in [22]. Indeed, similarly to outdoor conditions, the background was more than 5 m away for lighting experiments, while the back walls of the temperature-controlled rooms were less than 1 m away.

C. *Effect of Magnetic Fields*

Besides all natural environment considerations, magnetic fields are another factor typically influencing the scanning of energized power lines, as LineScout operates most of the time on energized conductors, with typical values of transiting loads being between 500 A and 1,000 A. The electronic parts and rotating motor inside the LIDAR may be affected by magnetic fields. To check this effect, a 40-m loop cable linked to a low-voltage current source is used. A specific intensity of current can thus be sent through the loop, creating a magnetic field of a specific magnitude. The LIDAR and targets were installed at a representative distance from the cable (0.6 m) and the LIDAR was set with its motor's axis of rotation in the following orientations relative to the cable: perpendicular, skewed, and parallel. Representative current levels ranging from 0 to 800 A were tested, producing a magnetic field of 149 µT, as measured with a Narda EFA-300 magnetic field analyzer. Presented in Figure 5, the results (at 800 A) are encouraging since neither orientation nor current level significantly affects distance measurements. Moreover, perceived diameter remains between 39.4 and 39.5 mm.

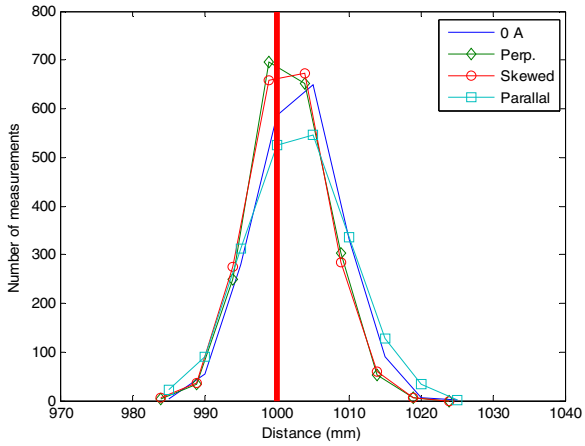

Figure 5. Effect of magnetic field on the distance measurement (800 A).

D. *Signal Intensity*

This section presents another parameter that can be used to detect obstacles: signal intensity. The UTM-30LX LIDAR can be configured to return this information by splitting the acquisition frequency in half: one complete scan returns distance values and the next returns intensity values (repeated alternately). The setup is the same as before except that tests were conducted at different incident angles for three cylindrical specimens with different surface finishes: a polished aluminum rod, a clean cable and an aged cable (see Figure 6). The resulting maximum intensities are presented in Figure 7.

Figure 6. Polished aluminum rod (left), clean cable (middle) and aged cable (right).

The surface finish clearly influences the maximum intensity measurement as all three specimens return different intensity values at all of the angles tested. This fact is more obvious when the laser beam is perpendicular to the surface (90º). Moreover, this parameter is also clearly influenced by the incident angle of the laser beam. Since an obstacle on a power line is seen as a change either in surface finish (multiple strands vs. smooth surface) or in surface orientation (edge of an obstacle), monitoring the return signal intensity could help obstacle detection.

Authorized licensed use limited to: Universidade Tecnologica Federal do Parana. Downloaded on January 22,2025 at 11:01:11 UTC from IEEE Xplore. Restrictions apply.

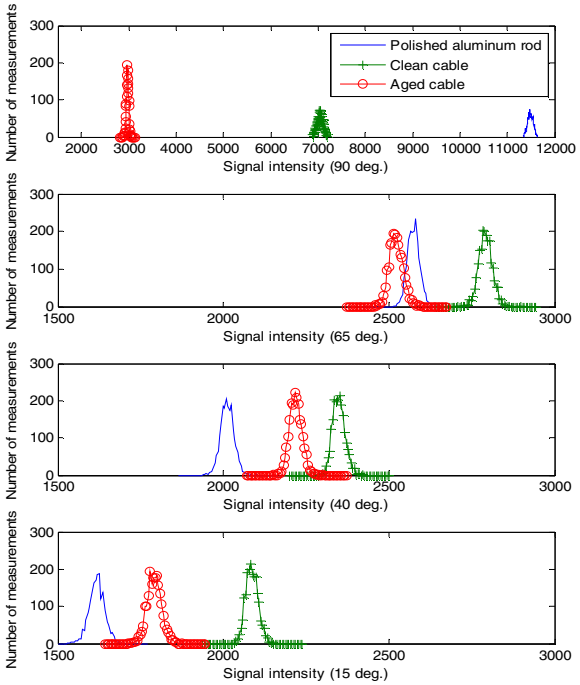

Figure 7. Effect of surface finish and incidence angle on return signal intensity.

To summarize, three parameters were studied to assist in obstacle detection. The distance measurement is more affected by temperature and lighting but still meets manufacturer specifications (< 10 mm). Perceived diameter decreases with a close background, while hot temperatures may increase LIDAR sensitivity. However, lighting and magnetic fields do not influence the perceived diameter. Another parameter, return signal intensity, may also be very useful in evaluating changes in orientation and type of scanned surfaces. Overall, the UTM-30LX LIDAR is expected to perform well in obstacle detection on power lines since most obstacles are quite unlike the cable, either in shape, surface finish or both. Although compensation with sensors (temperature, lighting etc.) would be interesting, following method takes into account parameters variations.

II. Obstacle Detection and Identification

The preceding section characterized the UTM-30LX LIDAR under typical conditions in the power line environment and helped find the conditions most affecting sensor measurement precision. This section focuses on detecting obstacles on power lines and determining thresholds for such detection.

A. Determining Detection Thresholds

In order to evaluate obstacles reliably, thresholds must be set for the parameters studied. Since environmental conditions are not always stable, the latest updated values at each scan must be compared to values for a calibrated cable section. The preceding sections showed that distance and signal intensity measurements follow a normal distribution, hence the means and the standard deviations can be evaluated and $\mu + 3\sigma$ can be used as valid thresholds.

Perceived diameter depends on the number of times the laser hits the target and boundary detection may be sensitive to small movements. In all of the preceding tests, the targets were not moving so the same region was systematically scanned. However, since cables are composed of multiple strands, the scanned surface is irregular and this may affect the perceived diameter evaluated during LineScout displacements due to small movements. Bearing in mind that the perceived diameter may be used as a detection criterion, it is important to assess its stability with a moving target.

To verify this, a clean cable specimen was hung on a rope 0.5 m long at a distance of 1 m from the LIDAR. This pendulum was subjected successively to three small movements: rotation around the cable's axis, oscillations in a plane located 1 m away from LIDAR's axis (left-right movement) and oscillations in a plane intersecting LIDAR's axis (forward-backward movement). Oscillations were initiated at 3 degrees and the natural frequency was about 4 rad/s. Rotations were induced by twisting the rope by 5 turns before releasing the specimen.

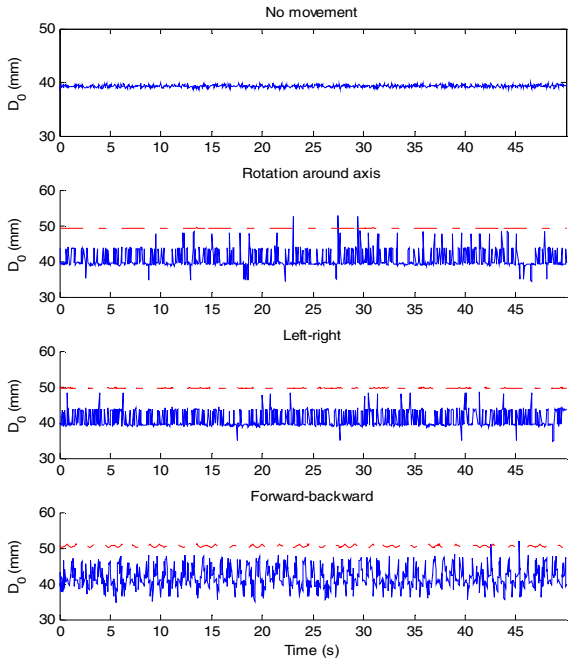

Figure 8. Effect of small movements on the perceived diameter (red dotted lines are thresholds) .

Based on the two middle graphs of Figure 8, it appears that the variation in perceived diameter is mainly due to the number of times the laser hits the cable. At 1 m, resolution r is 4.4 mm, which explains the many peaks at this amplitude. On the bottom graph, the diameter is influenced more by variations in the distance measurement. However, the mean perceived diameter does not change significantly since values are respectively 39.3, 40.5, 40.9 and 41.8 mm.

Given such oscillations, a threshold must be set to identify reliably a meaningful variation (due to an obstacle and not to noise) when using the perceived diameter as a criterion. Table I presents two proposed thresholds and gives the percentage of points included. One sets the threshold to the mean plus three times the standard deviation ($\mu + 3\sigma$),

Authorized licensed use limited to: Universidade Tecnologica Federal do Parana. Downloaded on January 22,2025 at 11:01:11 UTC from IEEE Xplore. Restrictions apply.

while the other sets it to the mean plus twice the linear resolution of the LIDAR at the perceived distance ($\mu + 2r_i$, i is the scan). In Figure 8, the red dotted line indicates the thresholds, showing that most peaks are within twice linear resolution r_i.

TABLE I. PERFORMANCE ASSOCIATED WITH EACH THRESHOLD

Movement	3σ (% of points)	$2r_i$ (% of points)
Rotation	97.9	99.7
Left-right	98.4	100
Forward-backward	99.8	99.8

Even though the data does not form a perfect normal distribution, a threshold of 3σ (< 8.7 mm) includes most of the data, although $2r$ is more effective (around 8.8 mm, depending on the perceived distance). Peaks above these thresholds still do exist, however, and cannot be rejected since they could indicate a splice. Subsection B explains how to deal with these peaks.

B. *Obstacle Detection*

To prove the feasibility of detecting obstacles on power lines using the UTM-30LX LIDAR, the latter was mounted on a simple PLR, called the LineROVer (Figure 9).

Figure 9. UTM-30LX mounted on the LineROVer.

To validate feasibility, tests must be conducted under difficult conditions, i.e., at high speed, in direct sunlight, at high temperature (~30ºC) and with the small incidence angle of 25 degrees (45 degrees is also tested for comparison). LineROVer was traveling at 0.64 m/s on a line approaching three obstacles: a splice, a clamp and a vibration damper. Although more obstacles can be encountered on conductors, these three are very representative and include the most challenging to detect, the splice. In fact, based on sensor angular resolution, broken strands could theoretically be detected, but further testing will be required. For the selected obstacles, the three parameters presented earlier were measured in order to determine which one(s) should be used to quickly detect a variation due to an obstacle.

Data for the cable before the obstacles were used to set the thresholds for the perceived diameter ($2r_i$), for the perceived distance (3σ) and for signal intensity.

Figure 10 plots the difference between measured data and calibration mean data for a 25-degree scan angle. Using the thresholds defined earlier, points associated with obstacle detection are highlighted in the same figure.

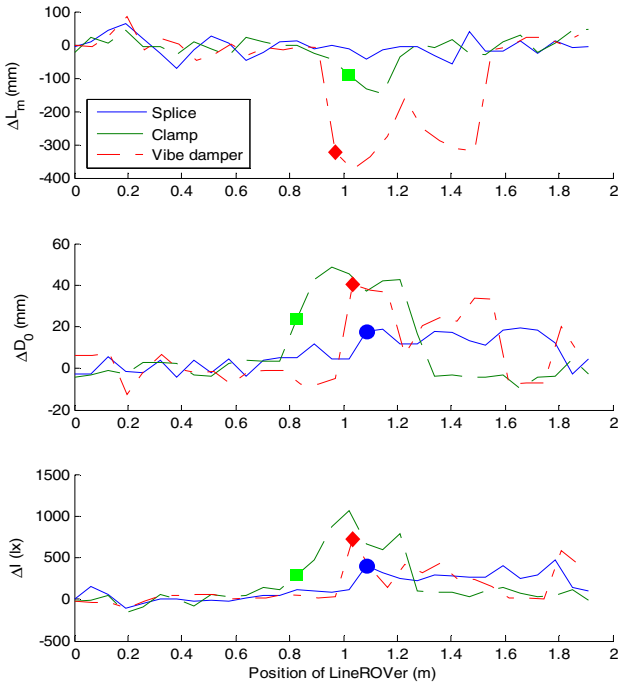

Figure 10. Obstacle detection based on distance, diameter and intensity variations relative to the conductor (scanning at 25 deg. and 0.64 m/s).

One important observation can be made from a glance at the graphs: all obstacles are detected using some or all the measured parameters. Based on this initial approach, the perceived diameter seems to be the most sensitive criterion since it is almost always the first to trigger detection, though it also depends on the shape of the obstacle. Also, perceived distance cannot be used to detect splices since the distance error overlaps the LIDAR's measurement threshold under these environmental conditions (mainly due to the sunlight and the high temperature, which increase σ).

If undesirable peaks exist and to avoid false detection, techniques can be used to ensure that an obstacle is really there so LineScout is not stopped needlessly. For example, the following algorithm seeks confirmation from at least one other criterion in either the same or the next scan (subscript *th* is for "threshold"):

1. if $D_0 > D_{0_{th}} \wedge L_m > L_{m_{th}} \wedge I > I_{th} \rightarrow$ STOP

   or

   if $D_0 > D_{0_{th}} \wedge L_m > L_{m_{th}} \rightarrow$ STOP

   or

   if $D_0 > D_{0_{th}} \wedge I > I_{th} \rightarrow$ STOP

   or

   if $L_m > L_{m_{th}} \wedge I > I_{th} \rightarrow$ STOP

Authorized licensed use limited to: Universidade Tecnologica Federal do Parana. Downloaded on January 22,2025 at 11:01:11 UTC from IEEE Xplore. Restrictions apply.

2. if $D_0 > D_{0_{th}} \rightarrow$ Next scan, if $D_0 > D_{0_{th}} \rightarrow$ STOP

or

if $L_m > L_{m_{th}} \rightarrow$ Next scan, if $L_m > L_{m_{th}} \rightarrow$ STOP

or

if $I > I_{th} \rightarrow$ Next scan, if $I > I_{th} \rightarrow$ STOP

This two-step detection process may result in a delay, which varies according to the number of scans needed to obtain confirmation. To quantify this delay, Table II assigns the value of 0.00 to LineScout's position when the first criterion exceeds its threshold and evaluates the distance traveled at full speed before detection is confirmed by a second criterion.

TABLE II. DETECTION DELAYS FOR THREE OBSTACLES (IN METERS)

Obstacle	Scan at 45 deg.			Scan at 25 deg.		
	L_m	D_0	I	L_m	D_0	I
Splice	-	-	**0.06**	-	**0.00**	**0.00**
Clamp	-	**0.00**	**0.00**	-	**0.00**	**0.00**
V. damper	**0.00**	**0.00**	-	**0.00**	**0.00**	-

Such results are promising since two criteria vary in the same scan most of the time. Moreover, delays are not excessive considering that braking tests show that LineScout needs 0.7 m to stop when traveling at top speed and that scanning at 25 deg. corresponds to a distance of 1.25 m in front of the robot. Overall, data collected with the UTM-30LX can be used to detect obstacles on power lines with very low software processing, i.e., data can be used practically directly based on the pre-computed thresholds.

III. EXPERIMENT ON POWER LINE MOCKUP

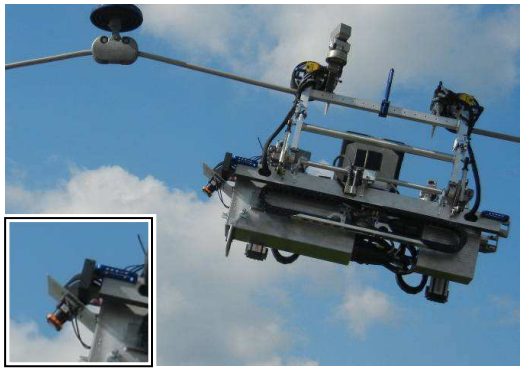

Figure 11. UTM-30LX on LineScout on a power line.

A final experiment was performed on a 2.5-km full-scale power line mockup. The UTM-30LX was mounted on LineScout, which then rolled up the cable until its cameras spotted the first clamp. It then advanced at a constant speed scanning the last section before the clamp (Figure 11).

On the way to the clamp, the entire 200 m length of cable was scanned at a 30-degree angle while moving at a speed of 0.91 m/s in order to calibrate and find usable thresholds. The data preceding the clamp is very interesting in that it shows that parameters can change slightly, primarily due to environmental conditions: winds reduce the LIDAR's temperature and cause slight LineScout movement, while the change in cable slope can affect the LIDAR's lighting conditions. Table III presents the means and standard deviations of the three parameters for the first 10 m of cable, the 10 m in the middle and the last 10 m before the clamp.

TABLE III. CHANGE IN PARAMETERS ALONG THE CABLE

Stats.	L_m		D_0		I	
	μ	σ	μ	σ	μ	σ
First 10 m	1.348	0.031	0.035	0.002	2886	110.5
Mid. 10 m	1.347	0.017	0.036	0.002	3090	85.0
Last 10 m	1.357	0.017	0.040	0.003	3163	74.8

It is noteworthy that all the parameters change slightly. This confirms that means and standard deviations must be re-evaluated regularly in order to detect meaningful variations. LineScout traveled at 0.15 and 0.30 m/s while scanning the clamp, giving the results presented in Figure 12.

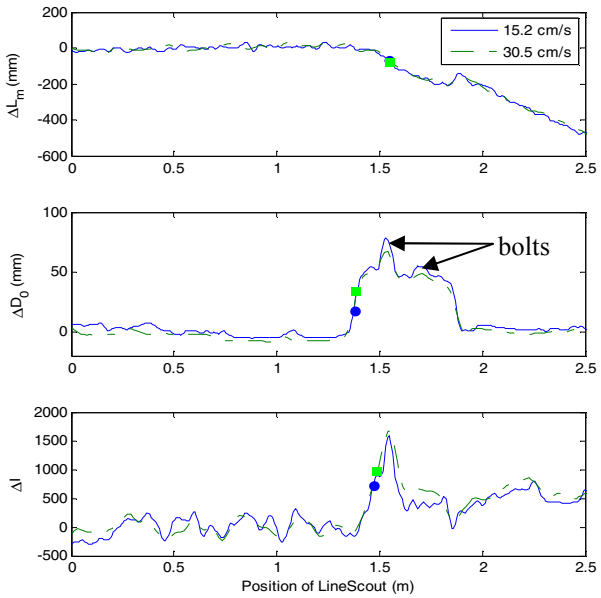

Figure 12. Variations of distance, diameter and intensity during a clamp scanning on a power line mockup (filtered).

All criteria clearly show the clamp. Moreover, the change in cable slope on the far side of the clamp can be perceived with the distance and intensity measurements. Even unexpected features could be perceived: attachment hardware was of non-standard length on the full-scale mockup as is evident in Figure 13. This clearly demonstrates the method's potential.

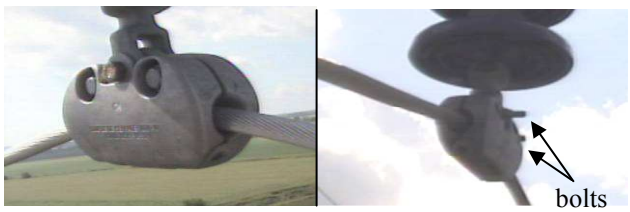

Figure 13. Clamp bolts detected.

Authorized licensed use limited to: Universidade Tecnologica Federal do Parana. Downloaded on January 22,2025 at 11:01:11 UTC from IEEE Xplore. Restrictions apply.

IV. CONCLUSION

This paper presented the first reported use of the Hokuyo UTM-30LX range finder on a power line robot. The sensor was first tested under the harsh conditions typical of a power line environment in order to verify how measurements would be affected. Temperature and lighting were the most influencing factors. Perceived diameter measurements were also tested with moving targets and provided specific detection thresholds for this criterion. Signal intensity experiments demonstrated the importance of the incidence angle and surface finish. Intensity was used as another detection criterion, along with perceived distance and diameter. The three criteria were tested using three common obstacles typically found on power lines: a splice, a clamp and a vibration damper. All three obstacles were shown to be detectable within one LIDAR scans (6 cm distance). Lastly, the UTM-30LX was mounted on LineScout for a field test on a full-scale power line mockup and detected a clamp with sufficient detail to reveal unexpected features, which appears very promising for the application.

Future work will mainly include background-related testing and the mounting a pair of Hokuyo UTM-30LX LIDARs on either ends of LineScout's frames. Servo-controlled pointing mechanisms will provide proper alignment of LIDAR scanning planes so that either of the units can perform obstacle detection or other dedicated scanning tasks. LIDAR signal control and processing based on the detection scheme presented will be performed by a 400-MHz sbRIO-9606 controller, which communicates in real time with LineScout's motherboard.

ACKNOWLEDGMENT

The authors would like to thank all development team members of the Institut de recherche d'Hydro-Québec (IREQ) and Hydro-Québec TransÉnergie personnel for their precious support.

REFERENCES

[1] Pascoal, J.; Marques, L.; de Almeida, A.T.; "Assessment of laser range finders in risky environments," Intelligent Robots and Systems, 2008. IROS 2008. IEEE/RSJ International Conference on, pp. 3533–3538, 22-26 Sept. 2008.

[2] Yeonsik K.; Chiwon R.; Seung-Beum S.; Bongsob S.; "A Lidar-based decision-making method for road boundary detection using multiple Kalman filters," Industrial Electronics, IEEE Transactions on, vol. 59, no. 11, pp. 4360–4368, Nov. 2012.

[3] Manz, M.; Himmelsbach, M.; Luettel, T.; Wuensche, H.; "Detection and tracking of road networks in rural terrain by fusing vision and LIDAR," Intelligent Robots and Systems (IROS), 2011 IEEE/RSJ International Conference on, pp. 4562–4568, 25-30 Sept. 2011.

[4] McDaniel, M.W.; Nishihata, T.; Brooks, C.A.; Iagnemma, K.; "Ground plane identification using LIDAR in forested environments," Robotics and Automation (ICRA), 2010 IEEE International Conference on, pp. 3831–3836, 3-7 May 2010.

[5] Cristiano P.; Oswaldo L.; Urbano N.; "LIDAR and vision-based pedestrian detection system," Journal of Field Robotics, vol. 26, no. 9, pp. 696–711, Sept. 2009.

[6] Chambers, A.; Achar, S.; Nuske, S.; Rehder, J.; Kitt, B.; Chamberlain, L.; Haines, J.; Scherer, S.; Singh, S.; "Perception for a river mapping robot," Intelligent Robots and Systems (IROS), 2011 IEEE/RSJ International Conference on, pp. 227–234, 25-30 Sept. 2011.

[7] Ulrich, W.; Biber, P.; "Plant detection and mapping for agricultural robots using a 3D LIDAR sensor," Robotics and Autonomous Systems, vol. 59, no. 5, pp. 265–273, May 2011.

[8] Gingras, D.; Lamarche, T.; Bedwani, J.-L.; Dupuis, E.; "Rough terrain reconstruction for rover motion planning," Computer and Robot Vision (CRV), 2010 Canadian Conference on, pp. 191–198, May 31, 2010-June 2, 2010.

[9] Toussaint, K.; Pouliot, N.; Montambault, S.; "Transmission line maintenance robots capable of crossing obstacles: State-of-the-art review and challenges ahead," Journal of Field Robotics, Wiley Ed., vol. 26, no. 5, pp. 477–499, May 2009.

[10] Peters, J. F.; Ramanna, S.; Szczuka, M. S.; "Towards a line-crawling robot obstacle classification system: A rough set approach," RSFDGrC 2003, LNAI 2639, pp. 303–307.

[11] Fu, S.; Li, W.; Zhang, Y.; Linag, Z.; Hou, Z.; Tan, M.; Ye, W.; Lian, B.; Zuo, Q.; "Structure-constrained obstacles recognition for power transmission line inspection robot", Proceedings of the 2006 IEEE/RSJ Int. Conference on Intelligent Robots and Systems, pp. 3363–3368, 9-15 Oct. 2006.

[12] Han, S.; Lee, J.; "Path-selection control of a power line inspection robot using sensor fusion," IEEE Int. Conf. on Multisensor Fusion and Integration for Intelligent Systems, pp. 8–13, Aug. 20-22, 2008.

[13] Qi, Z.; Zhi, X.; Zijian, G.; Dehui, S.; "The obstacle recognition approach for a power line inspection robot," Int. Conf. on Mechatronics and Automation ICMA 2009, pp. 1757–1761, Aug. 9-12, 2009.

[14] Wu, G.; Xu, X.; Xiao, H.; Dai, J.; Xiao, X.; Huang, Z.; Ruan, L.; Xiong, C.; Liu, H.; "A novel self-navigated inspection robot along high-voltage power transmission line and its application," ICIRA 2008, Springer Berlin / Heidelberg, pp. 1145–1154.

[15] Wang, L. et al., 2005, "Research on obstacle-navigation control of a mobile robot for inspection of the power transmission lines based on expert system," Proceedings of the 8th International Conference on Climbing and Walking Robots and the Support Technologies for Mobile Machines (CLAWAR 2005).

[16] Wu, G.; Zheng, T.; Huang, Z.; Liu, H.; Li, C.; "Navigation strategy for local autonomous obstacles-overcoming based on magnetic density detection for inspection robot of single split high voltage transmission line," 8th World Congress on Intelligent Control and Automation (WCICA), pp. 6555–6561, July 7-9, 2010.

[17] Pouliot, N.; Montambault, S.; "Geometric design of the LineScout, a teleoperated robot for power line inspection and maintenance," Proceedings of the IEEE International Conference on Robotics and Automation, ICRA 2008.

[18] Pouliot, N.; Latulippe, P.; Montambault, S.; Tremblay, S.; "Reliable and intuitive teleoperation of LineScout: a mobile robot for live transmission line maintenance," Proceedings of the IEEE/RSJ International Conference on Intelligent Robots and Systems, IROS 2009.

[19] Pouliot, N.; Montambault, S.; "Field-oriented developments for LineScout Technology and its deployment on large water crossing transmission lines," Journal of Field Robotics, vol. 29, no. 1, pp. 25–46, 2012.

[20] Pouliot, N.; Richard, P.-L.; Montambault, S., "LineScout power line robot: Characterization of a UTM-30LX LIDAR system for obstacle detection," Proceedings of the IEEE/RSJ International Conference on Intelligent Robots and Systems, IROS 2012.

[21] Jutila, J.; Kanna, K.; Visala, A., "Tree Measurement in Forest by 2D Laser Scanning," Proceedins of the IEEE International Symposium on Computational Intelligence in Robotics and Automation, CIRA 2007.

[22] Li, X.; Guang, M.; Hu, Y.; Li, W.; Jiang, Y.; Gong, J. Chen; H.; "Comparison of single-layer and multi-layer laser scanners for measuring characteristic," 2011, Applied Mechanics and Materials, vol. 128-129, pp. 548–552.

Authorized licensed use limited to: Universidade Tecnologica Federal do Parana. Downloaded on January 22,2025 at 11:01:11 UTC from IEEE Xplore. Restrictions apply.